XLIII CILAMCE
21–25, November, 2022
FOZ DO IGUAÇU – PR – BRAZIL

Reinforcements in Structural Masonry Prisms: A Numerical Study of Static and Dynamic Characteristics

Orlando M. L. Almeida[1], Orlando G. L. Almeida[1], Arlan A. Melo[1], Hidelbrando J. F. Diógenes[1], Joel A. N. Neto[2]

[1]*PPGECAM, Federal University of Paraíba - UFPB*
Campus Universitário, 58.051-900, João Pessoa/PB, Brazil
orlandomlalmeida@gmail.com, orlandogabriel96@gmail.com, arlan.melo@academico.ufpb.br, hjfd@academico.ufpb.br
[2]*Dept. of Civil Engineering, Federal University of Rio Grande do Norte - UFRN*
Campus Universitário, 59.078-970, Natal/RN, Brazil
joelneto@ct.ufrn.br

Abstract. Structural masonry is one of the oldest structural systems explored and currently has great relevance due to its economic competitiveness. Still, the need for structural reinforcement in this system is ever more common, either by restoring older structures or by changes in the behavior of static and dynamic loads on the systems. Thus, it becomes more necessary to know the dynamic characteristics of structural masonry walls, including those with structural reinforcements. This need occurs because of the wall's slenderness and also since these structures are subject to dynamic loads such as those caused by winds and earthquakes - which may be unforeseen additional loads due to recent changes in their territorial scope. Thus, this paper observes three different numerical models referring to concrete structural masonry prisms. The first type of prism was an Unreinforced Masonry (URM), the second was a Reinforced Masonry (RM) with a steel bar and grout, and the third type is reinforced by Fiber Reinforced Cementitious Matrix (FRCM). Therefore, the responses of the numerical models of the prisms to static loads were observed, using a load prediction for the models, in addition to an analysis of the vibration modes and the respective excitation frequencies.

Keywords: Masonry, Numerical Model, Reinforcement, Dynamic.

1 Introduction

Structural masonry is probably the first of the world's most known construction systems. Therefore, technological advances and changes in the environment impose greater intelligence on masonry structures' behavior - and applicable reinforcements - due to new load or material configurations.

According to Diógenes [1], the increase of skyscrapers, which elevates the incidence of wind loads, accentuates the relevance of a depth study of the material's dynamic properties.

Also, in agreement with Garcia-Ramonda et al. [2] scientific community's interest in retrofitting and repairing affected structures has grown after recent earthquakes.

In this context, Bayraktar et al. [3] state that the use of reinforcement on masonry walls changes its dynamic characteristics, and those variations might be favorable or not to the referred properties.

In this way, reinforced panels improve the wall's resistance even after fissuring. The panel withstands a good part of the load, allowing ductile rupture and greater damping of dynamic actions in accordance with Parsekian et al. [4].

In a recent study Meriggi et al. [5] propose a reinforcement for masonry walls that improves their in-plane strength, the fabric-reinforced cementitious matrix (FRCM), composed of high-strength fabrics that are attached to the masonry walls with the use of inorganic matrices.

In consonance with Garcia-Ramonda et al. [6] Fiber Reinforced Cementitious Matrix (FRCM) - known as Textile reinforced mortar (TRM) as well - has satisfactory compatibility with the wall subtract as an efficient

mechanical response.

Furthermore, according to Parsekian et al. [4], vertical steel bars embedded in grout along the masonry intern voids - Reinforced Masonry (RM) - can provide support capacity for gravitational and seismic loads and guarantee better ductility and tensile efficiency.

Tamboo et al. [7] state that the RM improves the axial load capacity due to the grout's high strength capacity. Also, the authors observed that the rebar embedded in the grout is well confined, improving its buckling strength and the whole model axial load capacity.

Additionally, in consonance with Asad et al. [8], lateral restrainers, although often used to prevent the steel bar from buckling, do not seem to influence the axial loading capacity or the masonry deformation. The grout around the bar provides enough support for buckling.

In this context, in agreement with Abdulla et al. [9], numerical models are considered a viable alternative to experimental programs, and the Finite Element Method (FEM) is one of the techniques adopted to simulate linear and non-linear behavior of masonry walls.

Then Rao [10] describes the FEM as replacing a complex problem with a simpler one. In this scenario, the solving body is considered composed of small, interconnected sub-bodies called finite elements. Also, according to the author, for each element, a convenient approximate solution is assumed as conditions for overall equilibrium are derived, then the satisfaction of those conditions outputs approximate stresses and displacements.

Also, according to Monteiro et al. [11], macro-modeling consists of a simple and practical approach to the FEM applied to masonry walls, this technique describes the wall as a homogenized model.

Thus, this paper developed numerical models based on FEM, using macro-modeling techniques for three groups of concrete masonry prisms: Unreinforced Masonry (URM), Reinforced Masonry (RM), and Fiber Reinforced Cementitious Matrix (FRCM).

2 Methodology

The present study was executed based on two main situations: axial compression and linear perturbation of the prisms. Each of them used the numerical model approach, with small variations for the second situation that will be described in the appropriate section.

2.1 Static Numerical Model

The model geometry was built on Abaqus® and based on the assembly of concrete block parts that had ABNT [12] as a basis. Each of the parts developed was considered deformable and tree-dimension, which will be discussed following.

The concrete blocks were conceded as solid parts created by the extrusion of a sketch. The material properties of this part were based on the Barbosa et al. [13] experiments for the elastic and plasticity behavior which was adopted as a Drucker Prager model. The mesh was composed of C3D8R (8-node linear brick 3D stress elements) in a total of 5643 elements for each concrete unit.

For the FRCM model, it was necessary to create a part for the steel fiber, which was created as a wire element with a 0,005m diameter and in two similar parts: Vertical and Horizontal Fiber. Its material was based on the commercial steel CA-60 mechanical properties for the elastic and plastic behavior. The element type used was a T3D2 (2-node linear 3-D truss) with a total of 29 elements for the horizontal fibers and 57 for the vertical ones. Booth wires were 0,05m spaced along with the prism's external surfaces.

In the RM model, the steel reinforcement was created as in the FRCM model, but corresponding to an area of a 0,01m diameter bar, and the material was based on commercial CA-50 mechanical properties. The element type is the T3D2 with 57 elements.

Also, for the RM, the grout was considered solid by extrusion, with elastic and plastic properties based on Peng et al. [14] and Marulanda et al. [15]. The element type chosen was the C3D8R, with a total of 4512 elements. A resume of the material properties adopted for each element can be observed in Tab. 1:

Table 1. Material Properties

Physical Quantity	Concrete	Steel Φ5	Steel Φ10	Grout
Elastic Modulus (GPa)	13	210	210	28.3
Poisson's ratio	0.2	0.3	0.3	0.25
Density (kg/m³)	2400	7800	7800	2100
Angle of Friction (º)	20	-	-	24
Flow Stress ratio	1	-	-	1
Dilation Angle (º)	30	-	-	25
Yield stress (MPa)	6.5	600	500	34
Ultimate stress (MPa)	17.1	660	550	56

Then, the models' interactions and constraints were set to represent the mortar behavior as the contact between grout, steel, and block. So, in order to simulate the mortar in between the blocks, the coefficients for friction, normal contact, and cohesion were applied based on Abdulla et al. [9]. The grout was considered tied to the units due to its high adhesion capacity, the steel bars were considered embedded in the grout, and the fibers were tied to the prism lateral surface. The interaction data for the mortar simulating can be found in Tab. 2:

Table 2. Interaction properties for mortar representation

Contact Property	Concrete Block	Value
Tangential Behavior	Penalty	0.75
Normal Behavior	Hard Contact	-
Cohesive Behavior	k_{nn} (N/m³)	6.3E+10
	k_{ss} (N/m³)	2.5E+10
	k_{tt} (N/m³)	2.5E+10

This way, the models' geometry could finally take place. The scheme for the URM, FRCM, and RM can be observed in Fig. 1.a to Fig. 1.c:

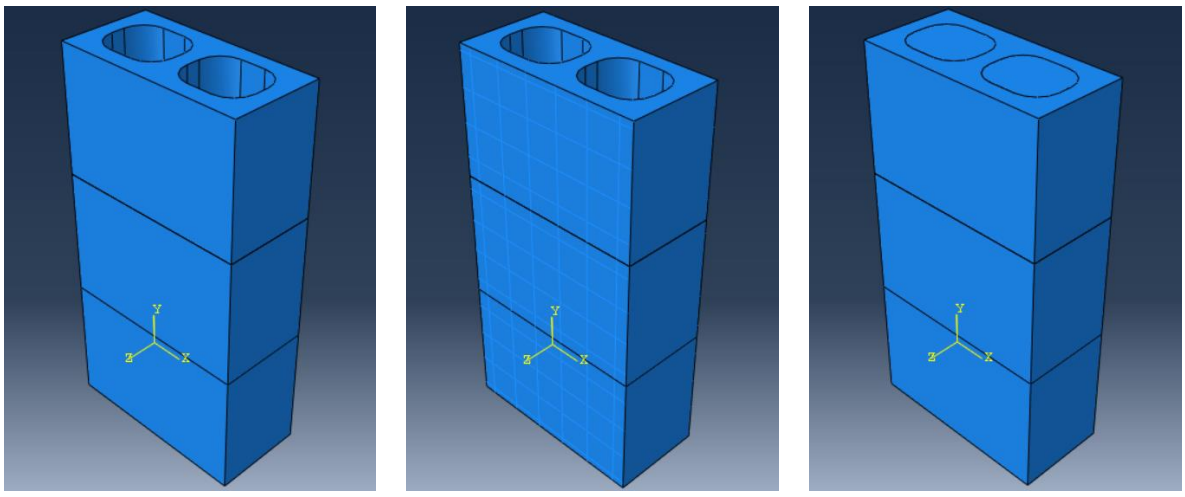

a. b. c.

Figure 1. Prisms Geometry: a. URM, b. FRCM, c. RM

Also, the step adopted was the general, static step. Its incrementation was set with an initial size of 0.0001, minimum of 1.0E-7, maximum of 0.01, and 1.0E+5 maximum number of increments. The Full Newton solution technique was chosen with ramp linearly load variation with time. To simulate the axial compression the prism base had each node considered Pinned as a boundary condition. Also, the pressure applied on the top of the prisms

had a total magnitude of 3E+5N based on Parsekian [16] load prediction. Then, the species were parallelly submitted to an axial displacement, and the top of the prism was pushed down to observe the models' collapse.

2.2 Dynamic Numerical Model

The dynamic models followed the static with some differences to accurate the structure behavior due to linear perturbation. First, the step was no longer "general static", as there would be no restriction to the movement on the boundary condition and no static load. Also, the interaction between the blocks was shifted to a tie constraint and the step was chosen as a linear perturbation (frequency), with a range of interest set from 50 to 3000 cycles per second. Lanczos as the selected solver to determine de eigenfrequencies and eigenvalues. Therefore, it is expected to analyze the reinforcements' impact on these structures' dynamic behavior.

3 Results

3.1 Static Model

After running the models under the 3E+5N load case, the material stresses were computed. At first, the tensions increased within the reinforcements because of the small steel area, results are shown in Fig. 2:

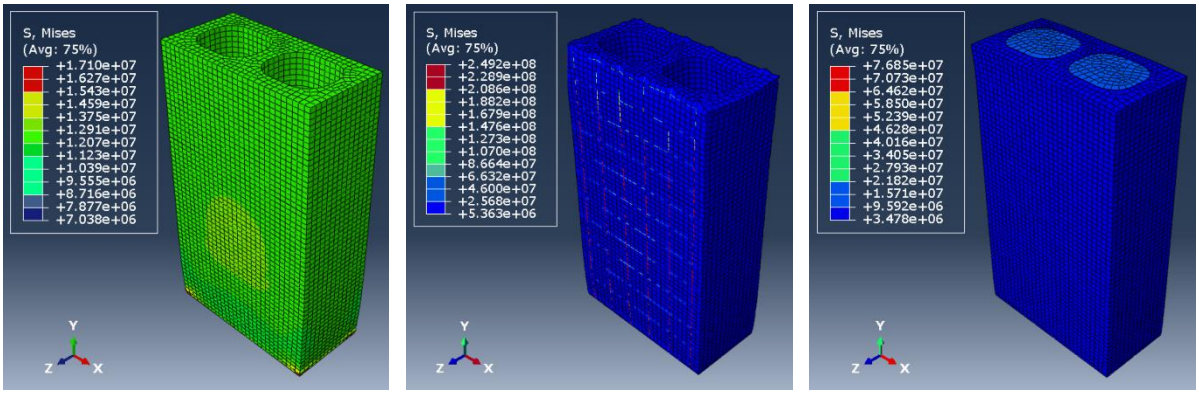

a. b. c.

Figure 2. Prisms stresses (Pa): a. URM, b. FRCM, c. RM

Also, the displacement in the y-axis (U2) decreased with the addition of the reinforcements. The displacement decreased 30.5% for the FRCM model and 78.2% for the RM due to the same load as shown in Fig. 3:

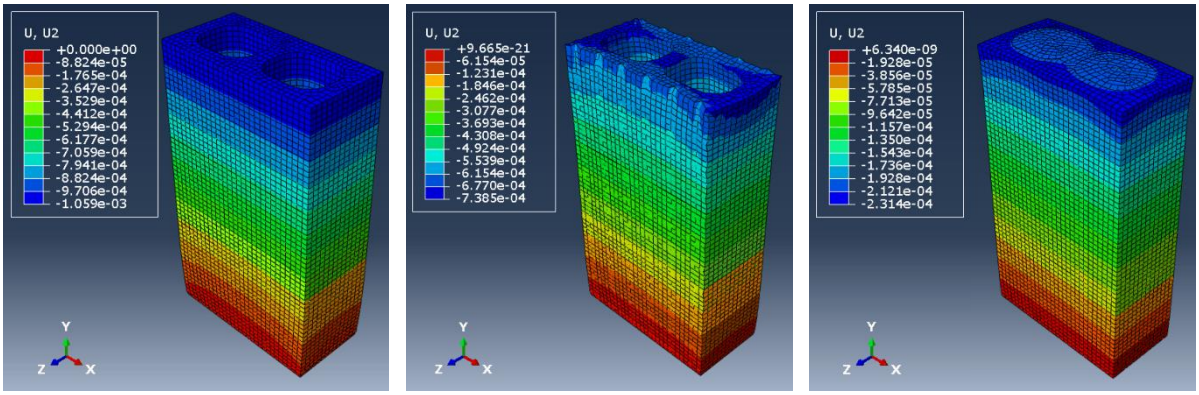

a. b. c.

Figure 3. Prisms displacement - U2 (m): a. URM, b. FRCM, c. RM

Then, the results for the stress-strain curve were obtained from the combination of the base elements' reaction forces in the y-direction sum and the average of the displacements in the y-direction of the top elements. With the referred data and using the block geometry (vertical length and cross-section liquid area) for each model. Also, the models' behavior under uniform axial displacement was observed as well in this analysis. The stress-strain curves were plotted as observed in Fig. 4:

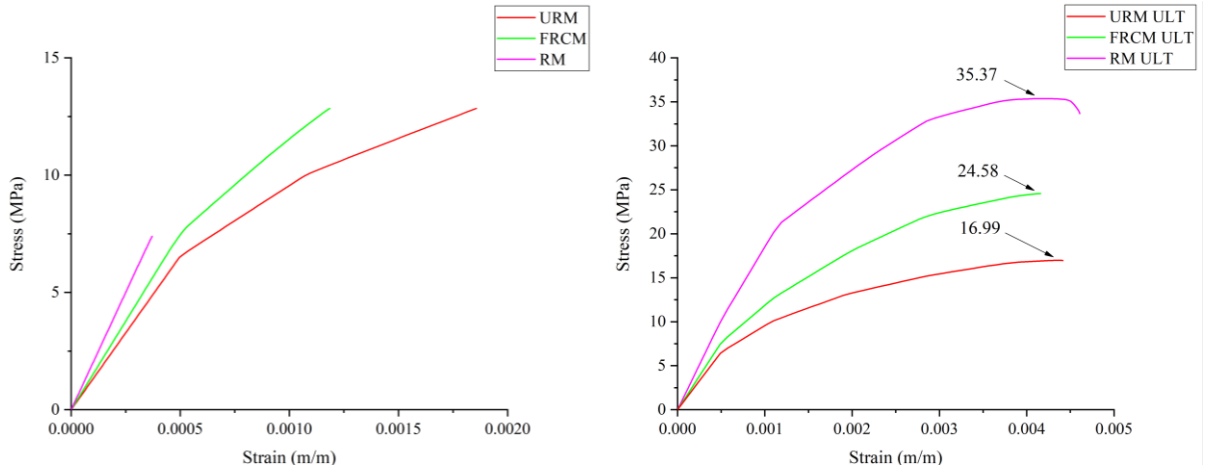

a. b.

Figure 4. Stress-strain model' curve: a. under 3E+5N load, b. under uniform 0.005m displacement

From the observed graph, the smaller stress applied to the RM while under the static load is explained since the section area increased with grout application. The total pressure supported by each model shows significant improvement in the FRCM, with an increase of 44%, and mainly in the RM, with a substantial gain of 108%.

3.2 Dynamic Model

The vibration modes observed vary slightly with the addition of the FRCM. The differences in the RM, when compared to the other models, are significant. Also, some vibration modes are restricted with the grout fill. In the specified range, the URM vibrates in 27 modes and the FRCM in 26 modes, yet the RM vibrates in only 8. This way, the comparison presented the same vibration modes for each model, even though the RM has fewer modes in the selected range. The equivalent vibration modes and frequencies are shown in Tab. 3:

Table 3. Vibration mode and Natural Frequencies

URM		FRCM		RM	
Vibration Mode	Frequency (Hz)	Vibration Mode	Frequency (Hz)	Vibration Mode	Frequency (Hz)
2	938.6	2	1015.3	1	976.1
5	1348.1	4	1362.7	3	1620.0
11	1827.8	11	1901.9	5	2240.6
13	2012.0	15	2106.2	6	2587.5

Then two examples of the model's behavior under the linear perturbation were selected, to begin it is observed the 1st transverse vibration mode, corresponding to the first row of Tab. 3. For this mode, is noted that the natural frequency becomes higher with both reinforcements, the FRCM had the greatest value as shown in Fig 5:

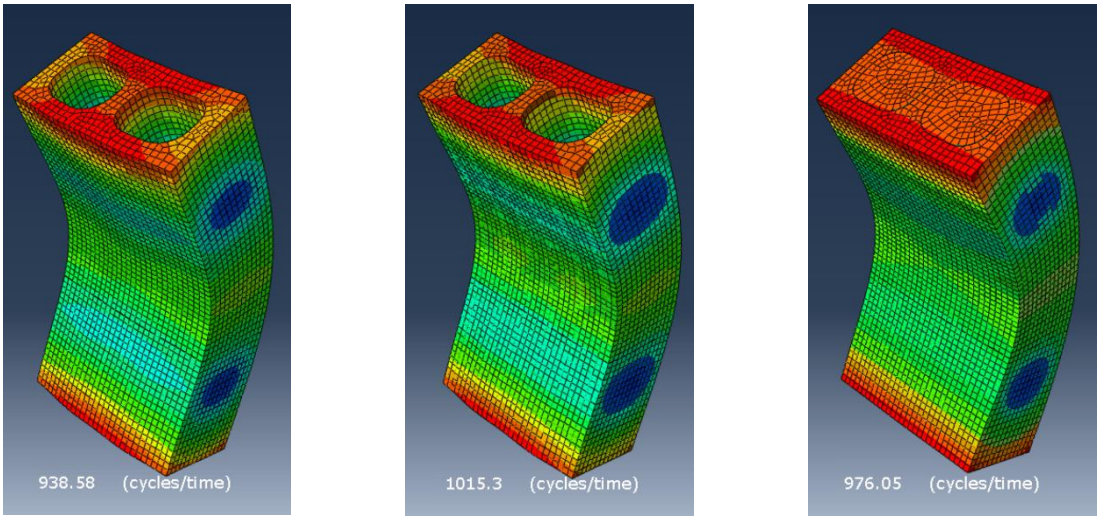

a. b. c.

Figure 5. Prisms 1st transverse vibration mode: a. URM, b. FRCM, c. RM

Also, it is possible to observe the 1st axial vibration mode, referred to in the last row of Tab. 3, where the natural frequency increases considerably, mainly to the RM. The cited vibration modes are plotted in Fig 6:

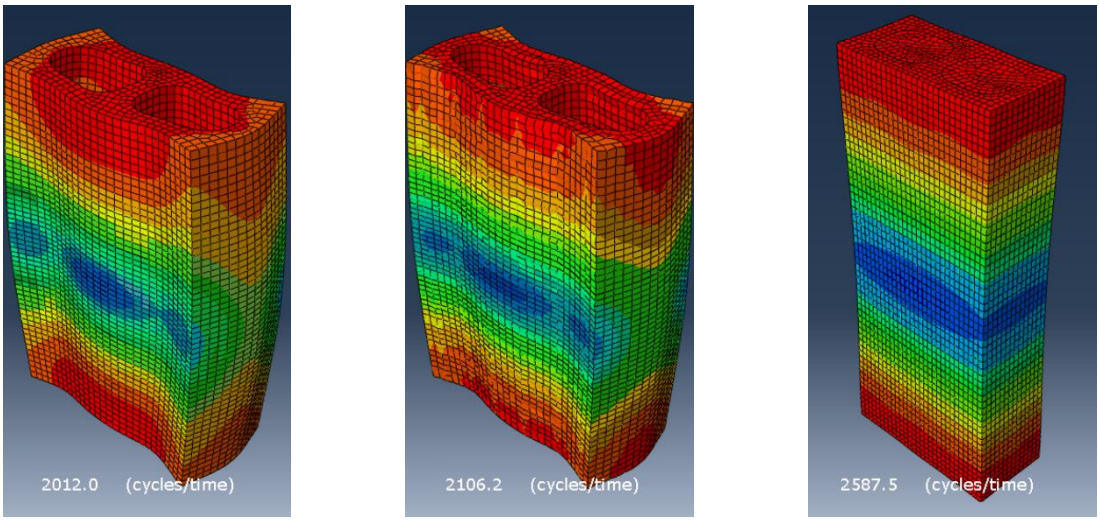

a. b. c.

Figure 6. Prisms 1st axial vibration mode: a. URM, b. FRCM, c. RM

Thus, the values for the natural frequencies increase with the use of FRCM and RM, also, those values tend to be even higher in the last one.

4 Conclusions

According to the numerical modeling adopted it was observed significant differences between the reinforced and unreinforced models. The static analysis showed that under the same applied load the prisms suffered less displacement when compared to the URM. The RM had not reached the yielding while the FRCM and URM were already under plastic deformation. The displacements decreased by 30.5% and 78.2% for the FRCM and RM,

respectively. Furthermore, the pressure capacity increase was substantial for the FRCM (44%) and for the RM (108%).

The dynamic analysis also demonstrated the effectiveness of both reinforcements in transposing the prism's natural frequency range, even though the FRCM interference was not as loud as the RM. The RM not only significantly increased the natural frequencies for the commo vibration modes but reduced the number of them from 27 to 8 vibration modes in the range adopted. That shift in the natural frequencies as the mitigation of the number of vibration modes can be interesting as a strategy to avoid specific vibration ranges.

The analysis indicates that FRCM and RM are plausible reinforcements depending on the environmental circumstances, although RM seems to be more effective due to the static and dynamic analysis adopted.

Acknowledgements. This study was financed in part by the Coordenação de Aperfeiçoamento de Pessoal de Nível Superior – Brasil (CAPES) – Finance Code 001. This study was supported by the Grupo de Pesquisa em Modelagem da Informação na Construção e Experimentação e Modelagem de Estruturas (MIMEE). This paper was subsidized by the computational software Abaqus®.

Authorship statement. The authors hereby confirm that they are the sole liable persons responsible for the authorship of this work, and that all material that has been herein included as part of the present paper is either the property (and authorship) of the authors, or has the permission of the owners to be included here.

References

[1] H.J.F. Diógenes. Análise tipológica de elementos e sistemas construtivos pré-moldados de concreto do ponto de vista de sensibilidade a vibrações de serviço. Masters degree dissertation, USP - Escola de Engenharia de São Carlos, 2010.
[2] L. Garcia-Ramonda, L. Pelà, P. Roca, G. Camata, "Cyclic shear-compression testing of brick masonry walls repaired and retrofitted with basalt textile reinforced mortar". *Composite Structures*, vol. 283, n. 115068, 2022.
[3] A. Bayraktar, İ. Çalik, T. Türker, A. Ashour, Restoration effects on experimental dynamic characteristics of masonry stone minarets, *Materials and Structures/Materiaux et Constructions*, vol. 51, n. 141, 2018.
[4] G.A. Parsekian, R.G. Drysdale, A.A. Hamid. *Comportamento e Dimensionamento de Alvenaria Estrutural*. Edufscar, 2012.
[5] P. Meriggi, S. de Santis, S. Fares, G. de Felice, "Design of the shear strengthening of masonry walls with fabric reinforced cementitious matrix". *Construction and Building Materials*, vol. 279, n. 122452, 2021.
[6] L. Garcia-Ramonda, L. Pelà, P. Roca, G. Camata, "Experimental cyclic behaviour of shear masonry walls reinforced with single and double layered Steel Reinforced Grout", *Construction and Building Materials*, vol. 320, n. 126053, 2022.
[7] J. Thamboo, T. Zahra, M. Asad, M. Song, "Improved design provisions for reinforced concrete block masonry walls under axial compression", *Construction and Building Materials*, vol. 310, n. 125226, 2021.
[8] M. Asad, T. Zahra, J. Thamboo, M. Song, "Finite element modelling of reinforced masonry walls under axial compression", *Engineering Structures*, vol. 252, n. 113594, 2022.
[9] K.F. Abdulla, L.S. Cunningham, M. Gillie, "Simulating masonry wall behaviour using a simplified micro-model approach", *Engineering Structures*, vol. 151, pp. 349-365, 2017.
[10] S.S. Rao. *The finite element method in engineering*. Elsevier/Butterworth Heinemann, 2004.
[11] A.C.L. Monteiro, K.K.F. Nunes, H.J.F. Diógenes, A.B. Silva, L.R.A. Costa, "Experimental and Numerical Study of Masonry with Emphasis on The Analysis of Structural Efficiency". In: Proceedings of the *XL Ibero-Latin-American Congress on Computational Methods in Engineering*, 2019.
[12] Associação Brasileira de Normas Técnicas – ABNT. *NBR 6136:2016 - Blocos vazados de concreto simples para alvenaria Requisitos*, 2016.
[13] C.S. Barbosa, J.B. Hanai, "Strength and deformability of hollow concrete blocks: correlation of block and cylindrical sample test results". *Ibracon structures and materials journal*, vol. 2, n. 1, pp. 85-99, 2009.
[14] G. Peng, X. Hu, D. Niu, S. Zhong, "Complete Stress-Strain Relations of Early-Aged Cementitious Grout under Compression: Experimental Study and Constitutive Model". *MDPI Materials*, vol. 15, n. 1238, 2022.
[15] Y. Marulanda, J. Vallejos, "Modeling the response of reinforcement elements during dynamic loading". *American rock mechanics association*, vol. 53, 2019.
[16] G.A. Parsekian. *Parâmetros de Projeto de alvenaria estrutural com blocos de concreto*. Edufscar, 2012.